SLAC–PUB–6560
October 1994
(T/E)

The Jet Cone Energy Fraction in e^+e^- Annihilation*

Y. Ohnishi

Department of Physics, Nagoya University
Nagoya 464, Japan

and

H. Masuda

Stanford Linear Accelerator Center
Stanford University, Stanford, CA 94309, U.S.A.

ABSTRACT

We present a new observable, the *Jet Cone Energy Fraction (JCEF)*, to characterize hadronic final states of e^+e^- annihilations. We studied the dependence of the $JCEF$ on the renormalization scale, hadronization effects, and the parton shower cutoff energy, compared with its sensitivity to the QCD scale parameter $\Lambda_{\overline{MS}}$. We also studied the reliability of the perturbative calculation of the $JCEF$.

Submitted to Physical Review D.

⋆ Work supported by Department of Energy contract DE–AC03–76SF00515.

Precise measurements of the strong coupling $\alpha_s(Q^2)$ at various energy scales Q are the key measurements for tests of the theory of strong interactions, Quantum Chromodynamics (QCD) [1]. In e^+e^- annihilation experiments, measurements of $\alpha_s(Q^2)$ have been performed over a wide energy range, from the τ lepton mass to the Z^0 boson mass, using a large number of infra-red and collinear safe observables which can be calculated by perturbative QCD. The experimental precision of the measurements has reached the 3% level in some cases [2,3,4,5,6]. However, the level of the total precision of $\alpha_s(M_Z^2)$ measurements is currently limited to about 5–10% by theoretical uncertainties, mainly due to the lack of higher order terms in perturbation theory and to the difficulties involved in calculations in the non-perturbative regime. The finite order perturbative QCD predictions of the observables depend on the *renormalization scale* μ which is often written in the form of the *renormalization scale factor* $f = \mu^2/Q^2$. It is an unphysical parameter, and exact predictions should not depend on it. In addition several pragmatic techniques, such as string fragmentation [7] and cluster fragmentation [8], are used to model the non-perturbative regime. In general the dependence on the unknown higher order contributions and the uncertainty in the non-perturbative regime are different for each observable, motivating the use of as many observables as possible. In particular it would be useful to find observables with relatively small dependence on these effects.

In this article we propose a new observable, the *Jet Cone Energy Fraction (JCEF)*, to characterize hadronic final states in e^+e^- annihilations. We estimate the effects of uncalculated higher order terms in the perturbative QCD series by changing the renormalization scale factor f. The uncertainty in the non-perturbative regime is estimated by comparing different hadronization models. We also estimate an additional theoretical uncertainty, which is closely correlated with both of the previous two uncertainties, by examining the dependence on the parton shower cutoff energy Q_0. In addition we investigate the range of applicability of the perturbative calculations of the $JCEF$. We have performed this study at the energy scale of $Q = M_Z$ (91.2 GeV). However, it is straightforward to extend our study to other energy scales.

We define the $JCEF$ to be the energy-weighted cross section for particle emission at a given angle with respect to the thrust axis. We first divide an event into two hemispheres by a plane perpendicular to the thrust axis. The invariant mass of each hemisphere is then calculated. The hemisphere which has larger invariant mass is called the heavy jet mass hemisphere, and the opposite hemisphere is called the light jet mass hemisphere. The direction of the thrust axis vector $\hat{n}_T$ is defined to point from the heavy jet mass hemisphere to the light jet mass hemisphere. The $JCEF$ is then defined by integrating energies which are included within a conical shell of opening angle χ around the thrust axis with thickness $\Delta\chi$,

$$JCEF(\chi) = \frac{1}{N_{events}\Delta\chi} \sum_{events} \int_{\chi-\frac{\Delta\chi}{2}}^{\chi+\frac{\Delta\chi}{2}} \sum_i \frac{E_i}{E_{vis}} \delta(\chi' - \chi_i) \mathrm{d}\chi', \qquad (1)$$

where E_i is the energy of a particle i, E_{vis} is the total visible energy in the event, and

$$\chi_i = \arccos\left(\frac{\vec{p}_i \cdot \hat{n}_T}{\mid \vec{p}_i \mid}\right) \qquad (2)$$

is the opening angle between a particle and $\hat{n}_T$. The half-angle χ of the cone is taken from $\chi = 0^\circ$ to $\chi = 180^\circ$.

The $JCEF$ has a perturbative QCD expansion up to $\mathcal{O}(\alpha_s^2)$ in the form,

$$JCEF(\chi) = \bar{a}A(\chi) + \bar{a}^2 B(\chi), \tag{3}$$

where $\bar{a} = \alpha_s/2\pi$, and the coefficients $A(\chi)$ and $B(\chi)$ can be calculated using the program `EVENT` [9]. We tabulated the coefficients $A(\chi)$ and $B(\chi)$ in 1.8° steps in Tables 1 and 2. Note that $A(\chi)$ is exactly zero in the light jet mass hemisphere ($0^\circ < \chi < 90^\circ$) due to a lack of first order contributions in this hemisphere. In other words hard gluon emission is dominant only in the heavy jet mass hemisphere ($90^\circ < \chi < 180^\circ$).

As we mentioned previously, perturbation theory in finite order does not specify the renormalization scale. Therefore we should consider the choice of the scale. Following the convention of Ref. [10], α_s is related to the QCD scale parameter $\Lambda_{\overline{MS}}$ in the modified minimal subtraction renormalization scheme [11] by

$$\alpha_s(\mu^2) = \frac{1}{b_0 \ln(\mu^2/\Lambda^2_{\overline{MS}})}\left[1 - \frac{b_1}{b_0^2}\frac{\ln\left[\ln(\mu^2/\Lambda^2_{\overline{MS}})\right]}{\ln(\mu^2/\Lambda^2_{\overline{MS}})}\right], \tag{4}$$

where $b_0 = (33-2n_f)/12\pi$, $b_1 = (153-19n_f)/24\pi^2$, and n_f is the number of active quark flavors. Here we have assumed the definition of $\Lambda_{\overline{MS}}$ for five active flavors. We should also account for the explicit dependence on μ in Eq. (3) by making the substitution

$$B(\chi) \longrightarrow B(\chi) + A(\chi)\cdot 2\pi b_0 \ln f, \tag{5}$$

from which we obtain the full expression

$$JCEF(\chi) = \bar{a}A(\chi) + \bar{a}^2[A(\chi) \cdot 2\pi b_0 \ln f \ + B(\chi)]. \tag{6}$$

Since $A(\chi)$ vanishes in the region of the light jet mass hemisphere, there are no terms contributing to the scale dependence in the $\mathcal{O}(\alpha_s^2)$ calculation for that hemisphere. To $\mathcal{O}(\alpha_s^2)$ the contributions in the light jet mass hemisphere are non-vanishing only for four-jet final states, which are calculated only at tree level. Therefore, in order to extract α_s reliably from a fit of the $JCEF$ calculated at $\mathcal{O}(\alpha_s^2)$, one should use the heavy jet mass hemisphere, $90° < \chi < 180°$. We need $\mathcal{O}(\alpha_s^3)$ terms to use the light jet mass hemisphere for reliable α_s measurements.

We first examine the renormalization scale dependence of the $JCEF$. Figure 1(a) shows the $JCEF$ for the renormalization scale factors $f = \mu^2/M_Z^2 = 0.01$, 0.1, 1.0, and 10 at $\Lambda_{\overline{MS}} = 200$ MeV, corresponding to $\alpha_s(M_Z^2) = 0.116$. Hereafter we use $\Lambda_{\overline{MS}} = 200$ MeV as the default value. Large differences can be seen in the light jet mass hemisphere in Fig. 1(a). These result from the different $\alpha_s(\mu^2)$ values at $f = 0.01$, 0.1, 1, and 10. In order to make a direct comparison of the dependence on f and $\Lambda_{\overline{MS}}$ in the heavy jet mass hemisphere, in which we are interested for α_s measurements, we consider the ratio of the $JCEF$ for each f and $\Lambda_{\overline{MS}}$ to that for the reference values $f = 1$ and $\Lambda_{\overline{MS}} = 200$ MeV. Figure 1(b) shows these ratios for $f = 0.01$, 0.1, and 10. Also shown are ratios for $\Delta\Lambda_{\overline{MS}} = \pm 50$ MeV and ± 100 MeV, where $\Delta\Lambda_{\overline{MS}}$ is the variation of $\Lambda_{\overline{MS}}$ value from 200 MeV. We can see that the deviations for $f = 0.1$ and 10 are within $\Delta\Lambda_{\overline{MS}} = \pm 100$ MeV for the region $110° < \chi < 170°$. This variation of $\Lambda_{\overline{MS}}$ corresponds to $\Delta\alpha_s/\alpha_s =^{+6.4}_{-9.3}$ %. Therefore we can expect that the scale dependence of $\Lambda_{\overline{MS}}$ within this fit range would be at most ± 100 MeV, if we consider the range $0.1 < f < 10$ for the estimation of scale dependence. However, for $f = 0.01$ the deviations are within $\Delta\Lambda_{\overline{MS}} = \pm 100$ MeV only within the more limited region of $120° < \chi < 160°$, and the scale dependence could be larger than ± 100 MeV if we consider the lower bound of f to be smaller than 0.01 with the same fit range as above.

Next we study the hadronization model dependence. To estimate the size of hadronization uncertainties, we use the JETSET 7.3 parton shower Monte Carlo with string fragmentation [7], and HERWIG 5.5 with cluster fragmentation [8] and study the difference in the size of the hadronization correction on the $JCEF$ between them. We used the default parameter values in each model. Figure 2(a) shows the $JCEF$ from these two models, and Fig. 2(b) shows the ratio of the HERWIG prediction to the JETSET prediction, compared with the ratios of theoretical predictions for $\Delta\Lambda_{\overline{MS}} = \pm 50$ MeV and ± 100 MeV. A large difference can be seen in the central angle region near the plane perpendicular to the thrust axis. Therefore one might want to exclude this region for α_s measurements. Fortunately this region is statistically insensitive to α_s measurements. The deviations are well within $\Delta\Lambda_{\overline{MS}} = \pm 50$ MeV except in the central angle region $70° < \chi < 110°$. This indicates that the hadronization uncertainty on $\alpha_s(M_Z^2)$ measurement from the $JCEF$ would be less than 4%, corresponding to $\Delta\Lambda_{\overline{MS}} = \pm 50$ MeV at most, assuming $\Lambda_{\overline{MS}} = 200$ MeV.

We now estimate the Q_0 dependence, where Q_0 is the parton shower cutoff energy [7]. This dependence arises both from the effects of uncalculated higher order terms and hadronization. Figure 3(a) shows the $JCEF$ from the JETSET predictions for $Q_0 = 0.5$, 1, 2, 4, and 8 GeV. Figure 3(b) shows the ratios of the

$JCEF$ for $Q_0 = 0.5$, 2, 4, and 8 GeV to that for $Q_0 = 1$ GeV which is the default value in this study, compared with the ratios for $\Delta\Lambda_{\overline{MS}} = \pm 50$ MeV and ± 100 MeV in Eq. (6). We can see from this figure that the Q_0 dependence in the heavy jet mass hemisphere is much smaller than that in the light one. This indicates that the contributions from uncalculated higher order terms are much more important in the latter, as expected. In the heavy jet mass hemisphere the deviations are well within $\Delta\Lambda_{\overline{MS}} = \pm 100$ MeV for all the cases in the angular region $110° < \chi < 170°$ and within ± 50 MeV for $0.5 < Q_0 < 2$ GeV in the same region.

Finally we investigate the reliability of the perturbative calculation of the $JCEF$ following the method proposed in Ref. [12]. We define $\mathcal{R}$ to be the ratio of the next-to-leading order (NLO) to leading order (LO) contributions to the $JCEF$,

$$\mathcal{R} = \frac{\bar{a}(A(\chi) \cdot 2\pi b_0 \ln f \ + B(\chi))}{A(\chi)}. \tag{7}$$

In general $\mathcal{R}$ depends on χ, $\Lambda_{\overline{MS}}$, and f. For a given set of $(\chi, \Lambda_{\overline{MS}}, f)$ the size of $\mathcal{R}$ gives an indication of the reliability of the calculation. If $|\mathcal{R}| \gtrsim 1$, the perturbation series shows no sign of convergence and we have no reason to hope that the uncalculated higher order terms are small. Furthermore, if $\mathcal{R} < -1$, $JCEF < 0$, which is unphysical. Equivalently, a given range of $\mathcal{R}$ defines a domain in $(\chi, \Lambda_{\overline{MS}}, f)$ within which the calculation is convergent to the stated level.

We calculate the range of f within which $|\mathcal{R}(\Lambda_{\overline{MS}}, f)| \leq \epsilon$ is satisfied. Figure 4 shows the range of f for $\epsilon = 0^\dagger$, 0.25, 0.5, and 1.0 as a function of χ at $\Lambda_{\overline{MS}} = 200$ MeV. The error bars on the histograms for $\epsilon = \pm 0.25$ indicate the

† The scale defined by this criterion corresponds to that resulting from the 'fastest apparent convergence' scale optimization prescription [13].

sizes of the differences corresponding to $\Delta\Lambda_{\overline{MS}} = 100$ MeV. We can see from this figure that the allowed f ranges depend on χ. They are rather stable for the region $100^\circ < \chi < 170^\circ$ but change rapidly for $\chi \sim 90^\circ$ and $\sim 180^\circ$. In the following, we consider the region $100^\circ < \chi < 170^\circ$ for further investigation. For $\epsilon = 0$ the allowed f varies from $\sim 10^{-2}$ for $\chi \sim 100^\circ$ to $\sim 10^{-1}$ for $\chi \sim 170^\circ$. The allowed f ranges are $[10^{-3}$–$10^{-1}]$ to $[10^{-1}$–$10^{2}]$ for $\epsilon = 0.25$ and $[5 \times 10^{-4}$–$10]$ to $[10^{-2} - 10^{6}]$ for $\epsilon = 0.5$. If one were to perform a fit of the QCD prediction to data for the region $100^\circ < \chi < 170^\circ$ with a single value of f, $f \sim 10^{-1}$ would give the best fit since this f value is well contained within the allowed f range for the small ϵ value. On the other hand, for $f < 10^{-4}$, $\mathcal{R} < -1$ which implies that perturbative calculation of the $JCEF$ cannot be reliably applied at such small scales.

In conclusion, we have presented a new observable, the *Jet Cone Energy Fraction* in e^+e^- annihilation. This observable can be used to determine α_s in the heavy jet mass hemisphere. We examined the dependences on the renormalization scale and hadronization model as well as on the parton shower cutoff energy, and compared these with the sensitivity to $\Lambda_{\overline{MS}}$, at the energy scale $Q = M_Z$ (91. GeV). We found that the dependence on the renormalization scale corresponds to $\Delta\Lambda_{\overline{MS}} = \pm 100$ MeV; that on the hadronization model corresponds to $\Delta\Lambda_{\overline{MS}}$ within ± 50 MeV; and that on the parton shower cutoff energy Q_0 corresponds to $\Delta\Lambda_{\overline{MS}}$ within ± 50 MeV in the angular region $110^\circ < \chi < 170^\circ$. We also studied the reliability of the perturbative calculation of the $JCEF$ and found that only a restricted scale range gives a well convergent perturbative series. It is straightforward to extend our study to other energy scales.

We wish to thank P.N. Burrows and D. Muller for helpful support, comments, and suggestions for this analysis. We also thank S.D. Ellis and K. Kato for their comments relating to this analysis.

REFERENCES

1. H. Fritzsch, M. Gell-Mann and H. Leutwyler, Phys. Lett. **B47** (1973) 365, D.J. Gross and F. Wilczek, Phys. Rev. Lett. **30** (1973) 1343, H.D. Politzer, Phys. Rev. Lett. **30** (1973) 1346.
2. ALEPH Collab., D. Decamp *et al.*, Phys. Lett. **B284** (1992) 163.
3. L3 Collab., O. Adriani *et al.*, Phys. Lett. **B284** (1992) 471.
4. OPAL Collab., P.D. Acton *et al.*, Z. Phys. **C59** (1993) 1.
5. DELPHI Collab., P. Abreu *et al.*, Z. Phys. **C59** (1993) 21.
6. SLD Collab., K. Abe *et al.*, Phys. Rev. Lett. **71** (1993) 2528; SLAC–PUB–6451 (1994); to appear in Phys. Rev. **D**; SLAC–PUB–6641 (1994); submitted to Phys. Rev. **D**.
7. T. Sjöstrand and M. Bengtsson, Comp. Phys. Comm. **43** (1987) 367.
8. G. Marchesini *et al.*, Comp. Phys. Commun. **67** (1992) 465.
9. Z. Kunszt and P. Nason, Z Physics at LEP 1, CERN Report CERN 89–08, Vol. 1 eds. G. Altarelli, R. Kleiss and C. Verzegnassi, p. 373.
10. Review of Particle Properties, K. Hikasa *et al.*, Phys. Rev. **D45** (1992) III.54.
11. W.A. Bardeen *et al.* Phys. Rev. **D18** (1978) 3998.
12. P.N. Burrows and H. Masuda, SLAC–PUB–6394 (1994); to appear in Z. Phys. C.
13. G. Grunberg, Phys. Rev. **D29** (1984) 2315.

Figure captions

Figure. 1. a) The $JCEF$ for the renormalization scale factor $f = 0.01$, 0.1, 1.0, and 10, at $\Lambda_{\overline{MS}} = 200$ MeV corresponding to $\alpha_s(M_Z^2) = 0.116$. b) The ratios of the $JCEF$ in the heavy jet hemisphere, $90^\circ \leq \chi \leq 180^\circ$, for $f = 0.01$, 0.1, and 10 to that for $f = 1$ at $\Lambda_{\overline{MS}} = 200$ MeV compared with those of theoretical predictions for $\Delta\Lambda_{\overline{MS}} = \pm 50$MeV and ± 100MeV.

Figure 2. a) The $JCEF$ from a JETSET 7.3 parton shower with string fragmentation and a HERWIG 5.5 parton shower with cluster fragmentation. b) The ratios of the HERWIG predictions to JETSET predictions, compared with those of theoretical predictions for $\Delta\Lambda_{\overline{MS}} = \pm 50$ MeV and ± 100 MeV.

Figure 3. a) The $JCEF$ from JETSET 7.3 with $Q_0 = 0.5$, 1, 2, 4, and 8 GeV. b) The ratios of the JETSET predictions at $Q_0 = 0.5$, 2, 4, and 8 GeV to those at $Q_0 = 1$ GeV, compared with those of theoretical predictions for $\Delta\Lambda_{\overline{MS}} = \pm 50$ MeV and ± 100 MeV.

Figure 4. The range of f for which $|\mathcal{R}| \leq \epsilon$ for $\epsilon = 0$ (solid histogram), 0.25 (dark shaded area), 0.5 (medium shaded area), and 1.0 (light shaded area) as a function of angle χ at $\Lambda_{\overline{MS}} = 200$MeV. Error bars on histograms for $\epsilon = \pm 0.25$ indicate the sizes of differences corresponding to $\Delta\Lambda_{\overline{MS}} = \pm 100$ MeV.

Table Captions

Table 1: Coefficient of the $\alpha_s/(2\pi)$ term for the $JCEF$. Errors indicate the numerical precision from the limited number of trials in the `EVENT` program.

Table 2: Same as Table 1 but for the $(\alpha_s/(2\pi))^2$ term for the $JCEF$.

Table 1

χ(deg.)	$A \pm \Delta A(rad^{-1})$
90.9	0.16398 $\pm$ 0.00228
92.7	0.47487 $\pm$ 0.00382
94.5	0.75172 $\pm$ 0.00459
96.3	1.0159 $\pm$ 0.0052
98.1	1.2628 $\pm$ 0.0056
99.9	1.4948 $\pm$ 0.0061
101.7	1.7166 $\pm$ 0.0063
103.5	1.9263 $\pm$ 0.0066
105.3	2.1371 $\pm$ 0.0066
107.1	2.3526 $\pm$ 0.0070
108.9	2.5703 $\pm$ 0.0071
110.7	2.7766 $\pm$ 0.0074
112.5	2.9874 $\pm$ 0.0076
114.3	3.2355 $\pm$ 0.0077
116.1	3.4664 $\pm$ 0.0079
117.9	3.6979 $\pm$ 0.0082
119.7	3.9631 $\pm$ 0.0084
121.5	4.1522 $\pm$ 0.0088
123.3	4.2892 $\pm$ 0.0090
125.1	4.4679 $\pm$ 0.0093
126.9	4.6369 $\pm$ 0.0094
128.7	4.8409 $\pm$ 0.0100
130.5	5.0873 $\pm$ 0.0104
132.3	5.3039 $\pm$ 0.0109
134.1	5.5818 $\pm$ 0.0115
135.9	5.9072 $\pm$ 0.0119
137.7	6.2567 $\pm$ 0.0126
139.5	6.6520 $\pm$ 0.0135
141.3	7.0932 $\pm$ 0.0143
143.1	7.5688 $\pm$ 0.0151
144.9	8.1589 $\pm$ 0.0161
146.7	8.8522 $\pm$ 0.0176
148.5	9.6314 $\pm$ 0.0191
150.3	10.479 $\pm$ 0.0208
152.1	11.585 $\pm$ 0.0229
153.9	12.846 $\pm$ 0.026
155.7	14.324 $\pm$ 0.028
157.5	16.152 $\pm$ 0.032
159.3	18.352 $\pm$ 0.037
161.1	21.079 $\pm$ 0.042
162.9	24.683 $\pm$ 0.051
164.7	29.267 $\pm$ 0.060
166.5	35.340 $\pm$ 0.073
168.3	43.957 $\pm$ 0.091
170.1	56.431 $\pm$ 0.120
171.9	75.573 $\pm$ 0.168
173.7	108.52 $\pm$ 0.25
175.5	176.64 $\pm$ 0.43
177.3	363.77 $\pm$ 1.03
179.1	—

Table 2

χ(deg.)	$B \pm \Delta B (rad^{-1})$	χ(deg.)	$B \pm \Delta B (rad^{-1})$
0.9	—	90.9	8.2563 $\pm$ 0.898
2.7	14868. $\pm$ 217.0	92.7	15.258 $\pm$ 1.174
4.5	5338.3 $\pm$ 53.1	94.5	23.950 $\pm$ 1.281
6.3	2721.0 $\pm$ 18.9	96.3	27.021 $\pm$ 1.275
8.1	1633.5 $\pm$ 12.0	98.1	28.636 $\pm$ 1.137
9.9	1062.3 $\pm$ 5.7	99.9	31.885 $\pm$ 1.227
11.7	765.47 $\pm$ 10.58	101.7	35.449 $\pm$ 1.456
13.5	553.25 $\pm$ 3.00	103.5	35.415 $\pm$ 1.262
15.3	420.38 $\pm$ 2.06	105.3	41.253 $\pm$ 2.602
17.1	330.77 $\pm$ 1.81	107.1	39.855 $\pm$ 1.229
18.9	265.28 $\pm$ 1.41	108.9	41.161 $\pm$ 1.244
20.7	216.69 $\pm$ 1.09	110.7	43.677 $\pm$ 1.546
22.5	180.60 $\pm$ 1.38	112.5	44.456 $\pm$ 1.497
24.3	152.41 $\pm$ 2.36	114.3	42.645 $\pm$ 1.313
26.1	127.48 $\pm$ 0.49	116.1	46.702 $\pm$ 2.723
27.9	110.18 $\pm$ 0.51	117.9	42.445 $\pm$ 1.799
29.7	97.231 $\pm$ 1.637	119.7	44.209 $\pm$ 1.530
31.5	84.454 $\pm$ 0.366	121.5	45.258 $\pm$ 1.595
33.3	74.370 $\pm$ 0.281	123.3	47.315 $\pm$ 1.579
35.1	66.520 $\pm$ 0.251	125.1	48.696 $\pm$ 1.839
36.9	59.645 $\pm$ 0.253	126.9	57.055 $\pm$ 4.800
38.7	54.145 $\pm$ 0.239	128.7	60.734 $\pm$ 1.767
40.5	49.166 $\pm$ 0.340	130.5	62.452 $\pm$ 4.969
42.3	44.674 $\pm$ 0.158	132.3	60.275 $\pm$ 1.924
44.1	41.138 $\pm$ 0.166	134.1	65.203 $\pm$ 2.668
45.9	37.672 $\pm$ 0.133	135.9	69.156 $\pm$ 2.062
47.7	34.922 $\pm$ 0.112	137.7	70.474 $\pm$ 2.315
49.5	32.682 $\pm$ 0.127	139.5	76.031 $\pm$ 3.372
51.3	30.562 $\pm$ 0.129	141.3	76.776 $\pm$ 2.439
53.1	28.671 $\pm$ 0.133	143.1	88.579 $\pm$ 5.608
54.9	26.946 $\pm$ 0.101	144.9	95.569 $\pm$ 4.874
56.7	25.491 $\pm$ 0.091	146.7	89.324 $\pm$ 3.077
58.5	24.213 $\pm$ 0.099	148.5	101.36 $\pm$ 3.07
60.3	23.222 $\pm$ 0.109	150.3	102.62 $\pm$ 3.54
62.1	22.070 $\pm$ 0.065	152.1	107.49 $\pm$ 5.20
63.9	21.297 $\pm$ 0.112	153.9	116.60 $\pm$ 4.23
65.7	20.626 $\pm$ 0.112	155.7	125.54 $\pm$ 4.40
67.5	19.761 $\pm$ 0.065	157.5	137.57 $\pm$ 8.50
69.3	19.143 $\pm$ 0.071	159.3	127.03 $\pm$ 5.79
71.1	18.753 $\pm$ 0.068	161.1	145.93 $\pm$ 7.76
72.9	18.352 $\pm$ 0.051	162.9	130.81 $\pm$ 9.25
74.7	18.105 $\pm$ 0.051	164.7	137.62 $\pm$ 10.62
76.5	17.888 $\pm$ 0.048	166.5	123.53 $\pm$ 12.58
78.3	17.785 $\pm$ 0.062	168.3	55.268 $\pm$ 15.97
80.1	17.601 $\pm$ 0.064	170.1	-97.861 $\pm$ 23.28
81.9	17.223 $\pm$ 0.045	171.9	-260.64 $\pm$ 36.07
83.7	16.885 $\pm$ 0.065	173.7	-998.67 $\pm$ 49.64
85.5	16.238 $\pm$ 0.054	175.5	-2806.9 $\pm$ 170.6
87.3	14.410 $\pm$ 0.054	177.3	-11459.0 $\pm$ 338.0
89.1	9.0241 $\pm$ 0.042	179.1	—

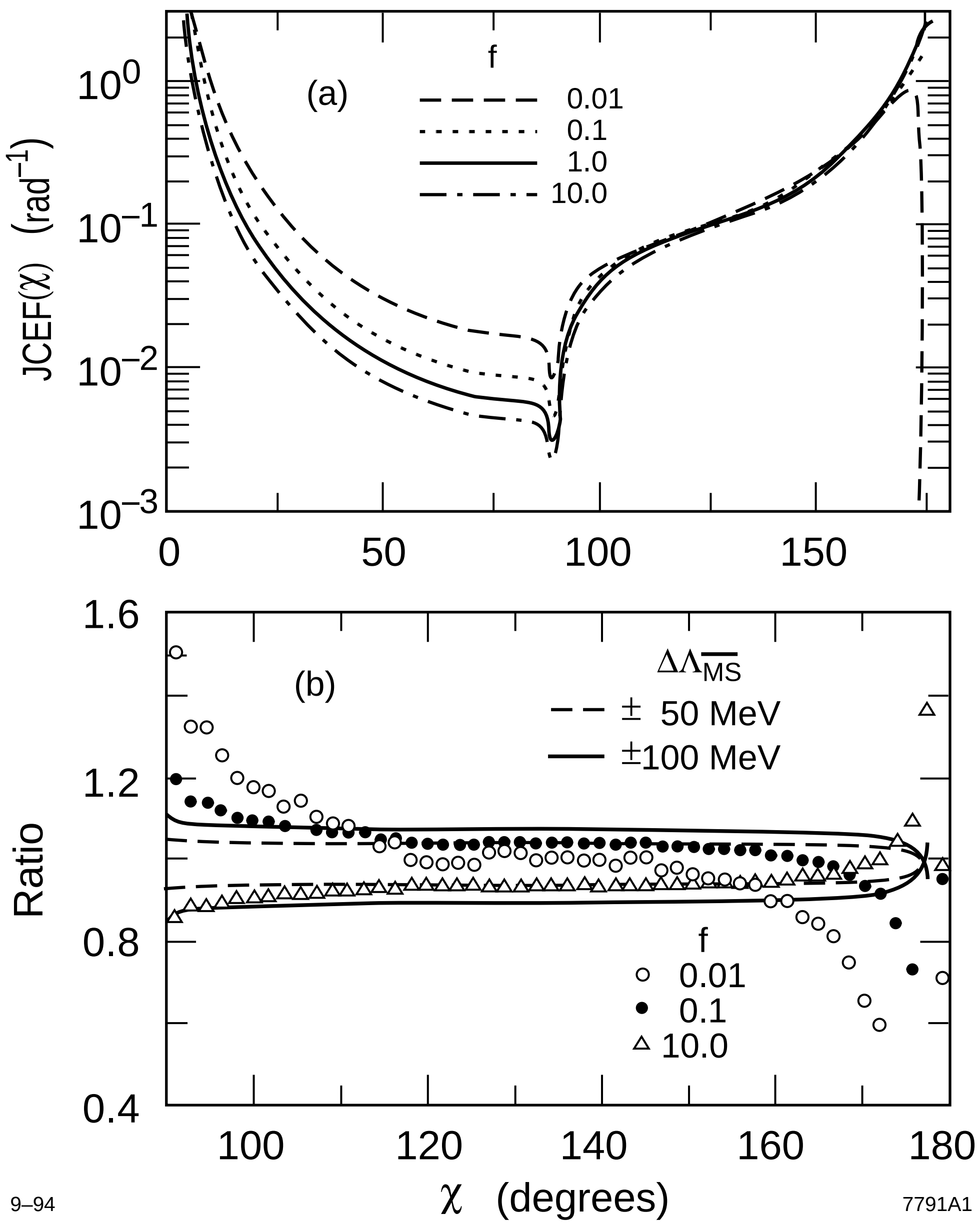
(a)
f
0.01
0.1
1.0
10.0
JCEF(χ) (rad⁻¹)
10⁰
10⁻¹
10⁻²
10⁻³
0
50
100
150
(b)
ΔΛ_MS
± 50 MeV
±100 MeV
Ratio
1.6
1.2
0.8
0.4
f
0.01
0.1
10.0
100
120
140
160
180
χ (degrees)
9–94
7791A1

Figure 1

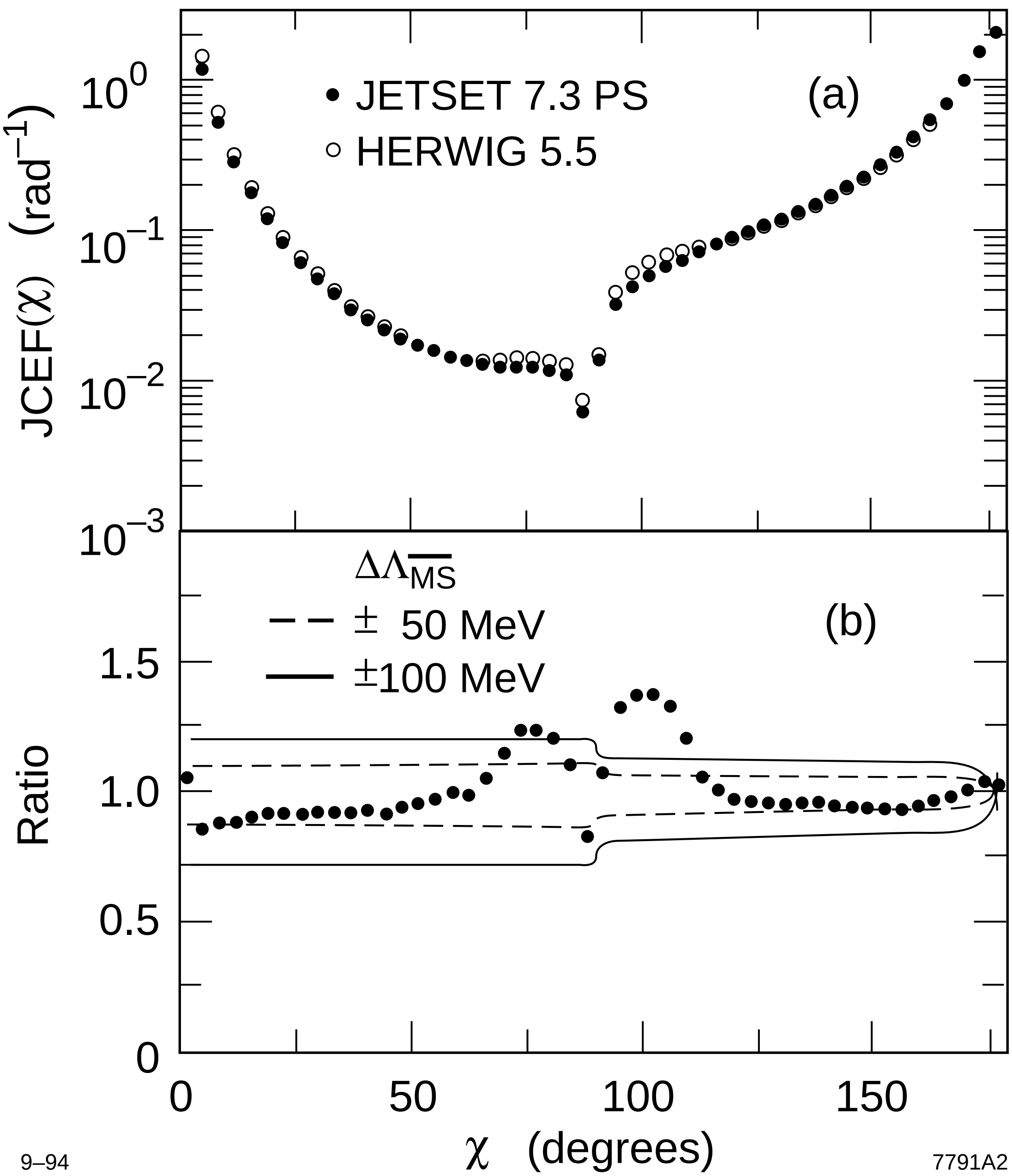

JETSET 7.3 PS
HERWIG 5.5
(a)
JCEF(χ) (rad^{-1})
10^0
10^{-1}
10^{-2}
10^{-3}
$\Delta\Lambda_{\overline{MS}}$
± 50 MeV
±100 MeV
(b)
Ratio
1.5
1.0
0.5
0
0
50
100
150
χ (degrees)
9–94
7791A2

Figure 2

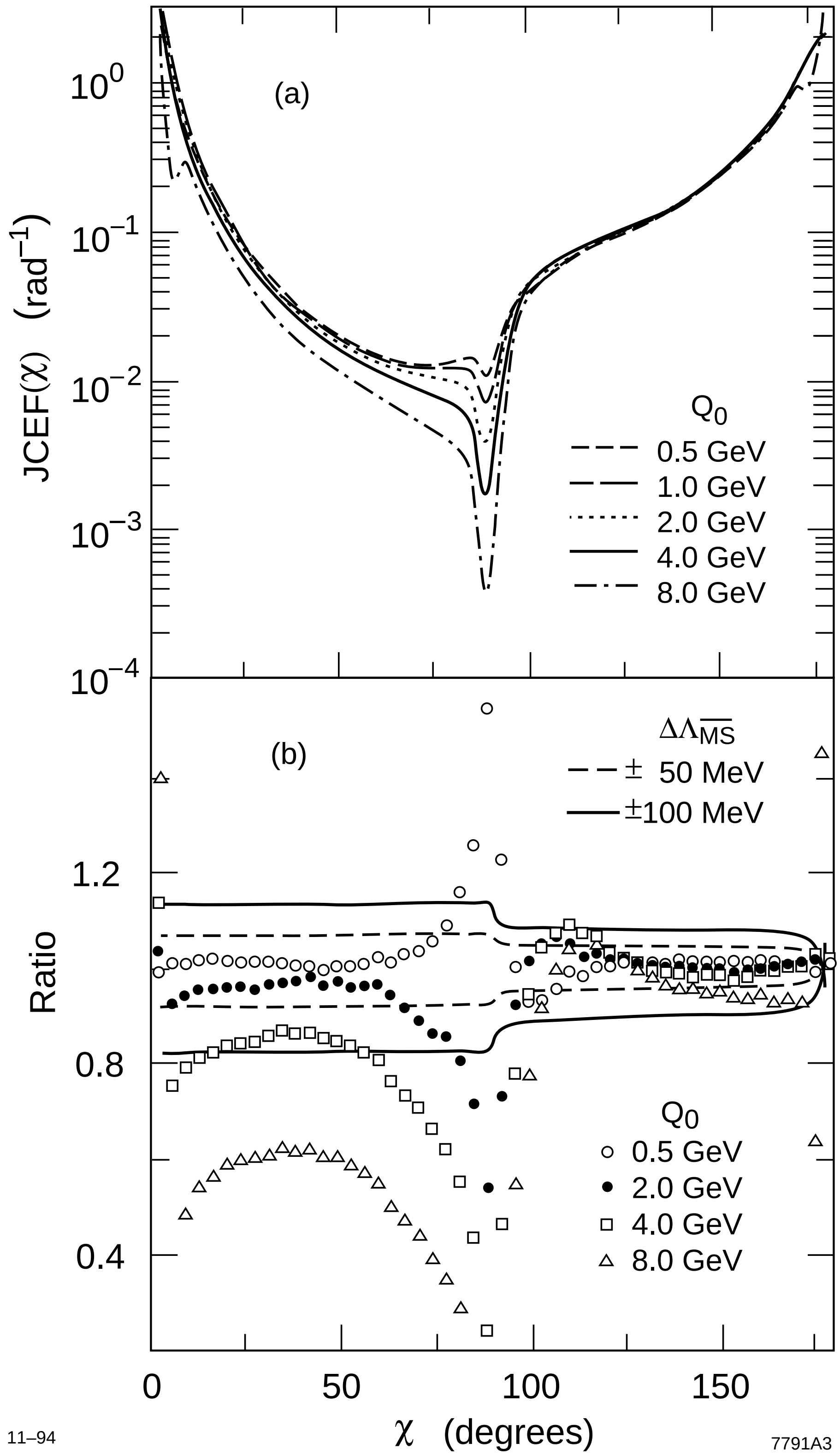

(a)
JCEF(χ) (rad^{-1})
10^0
10^{-1}
10^{-2}
10^{-3}
10^{-4}
Q_0
0.5 GeV
1.0 GeV
2.0 GeV
4.0 GeV
8.0 GeV
(b)
$\Delta\Lambda_{\overline{MS}}$
± 50 MeV
±100 MeV
Ratio
1.2
0.8
0.4
Q_0
0.5 GeV
2.0 GeV
4.0 GeV
8.0 GeV
0
50
100
150
χ (degrees)
11–94
7791A3

Figure 3

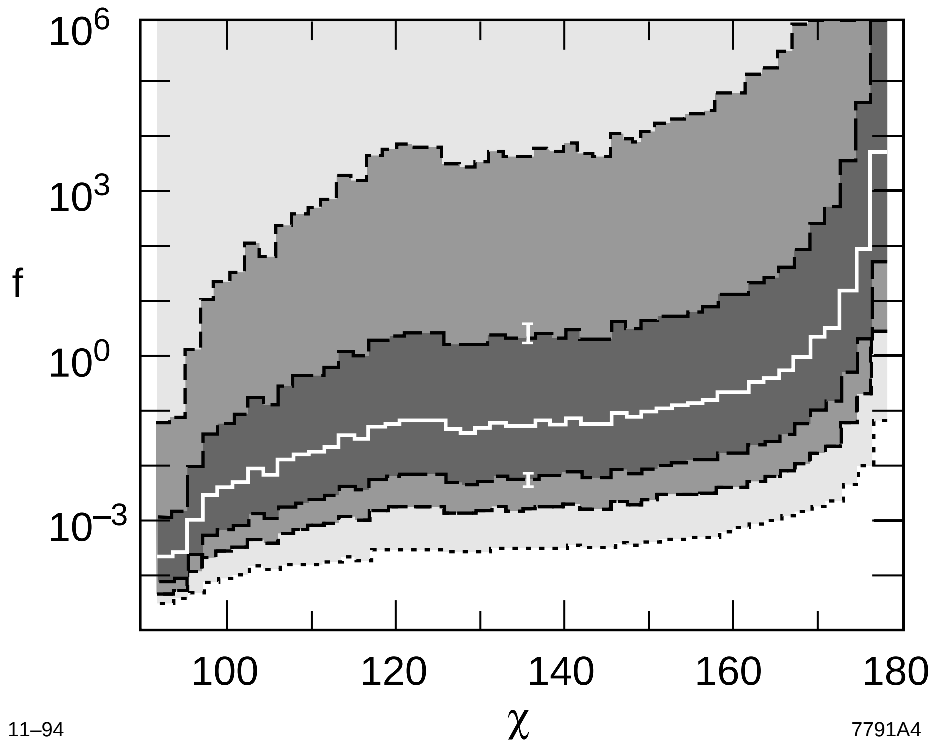

Figure 4

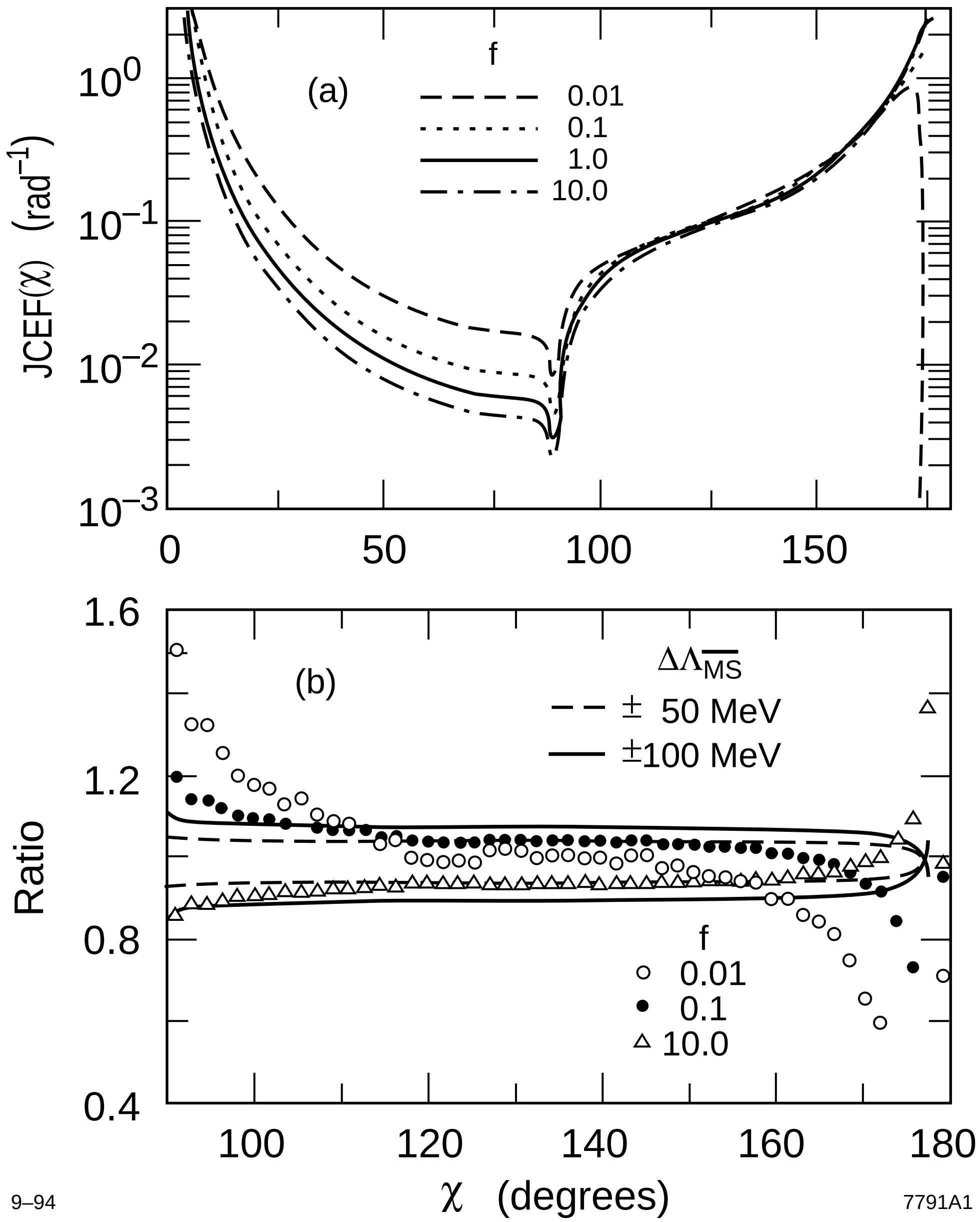
(a)
f
0.01
0.1
1.0
10.0
JCEF(χ) (rad⁻¹)
10^0
10^-1
10^-2
10^-3
0
50
100
150
(b)
ΔΛ_MS
± 50 MeV
±100 MeV
Ratio
1.6
1.2
0.8
0.4
f
0.01
0.1
10.0
100
120
140
160
180
9–94
χ (degrees)
7791A1

Figure 1

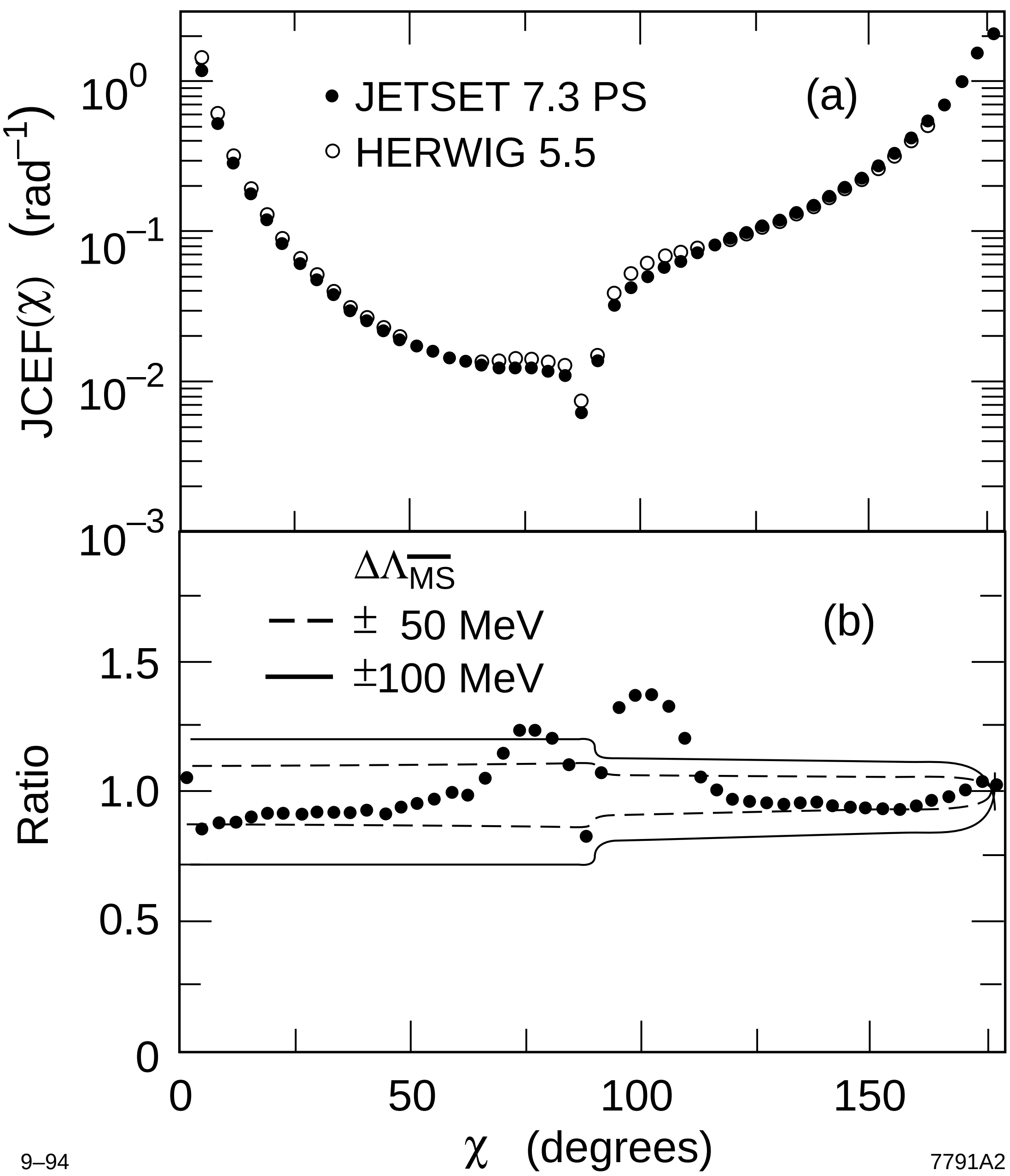

JCEF(χ) (rad^{-1})
10^0
10^{-1}
10^{-2}
10^{-3}
JETSET 7.3 PS
HERWIG 5.5
(a)
$\Delta\Lambda_{\overline{MS}}$
± 50 MeV
±100 MeV
(b)
Ratio
1.5
1.0
0.5
0
0
50
100
150
χ (degrees)
9–94
7791A2

Figure 2

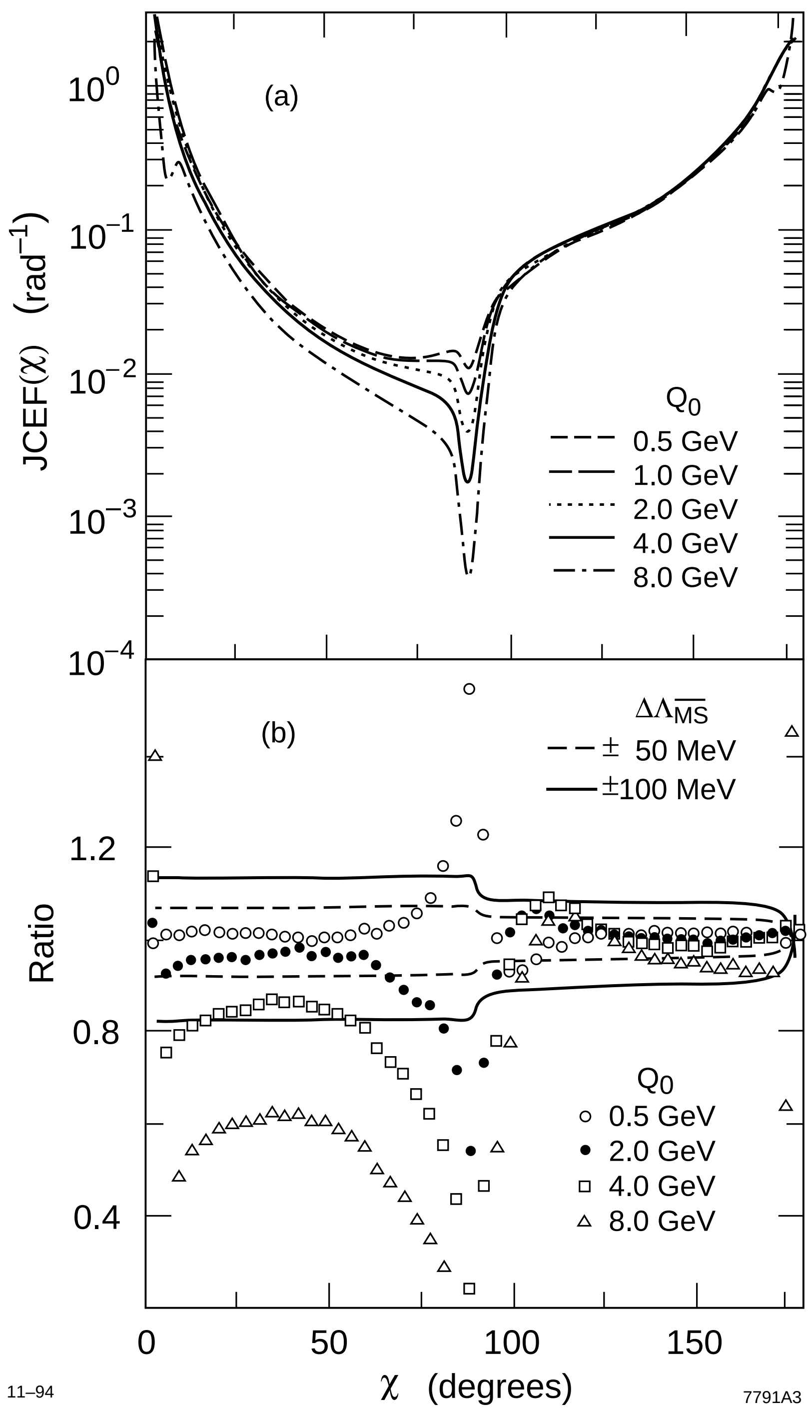
(a)
JCEF(χ) (rad^{-1})
10^0
10^{-1}
10^{-2}
10^{-3}
10^{-4}
Q_0
0.5 GeV
1.0 GeV
2.0 GeV
4.0 GeV
8.0 GeV
(b)
$\Delta\Lambda_{\overline{MS}}$
± 50 MeV
±100 MeV
Ratio
1.2
0.8
0.4
Q_0
0.5 GeV
2.0 GeV
4.0 GeV
8.0 GeV
0
50
100
150
χ (degrees)
11–94
7791A3

Fig. 3

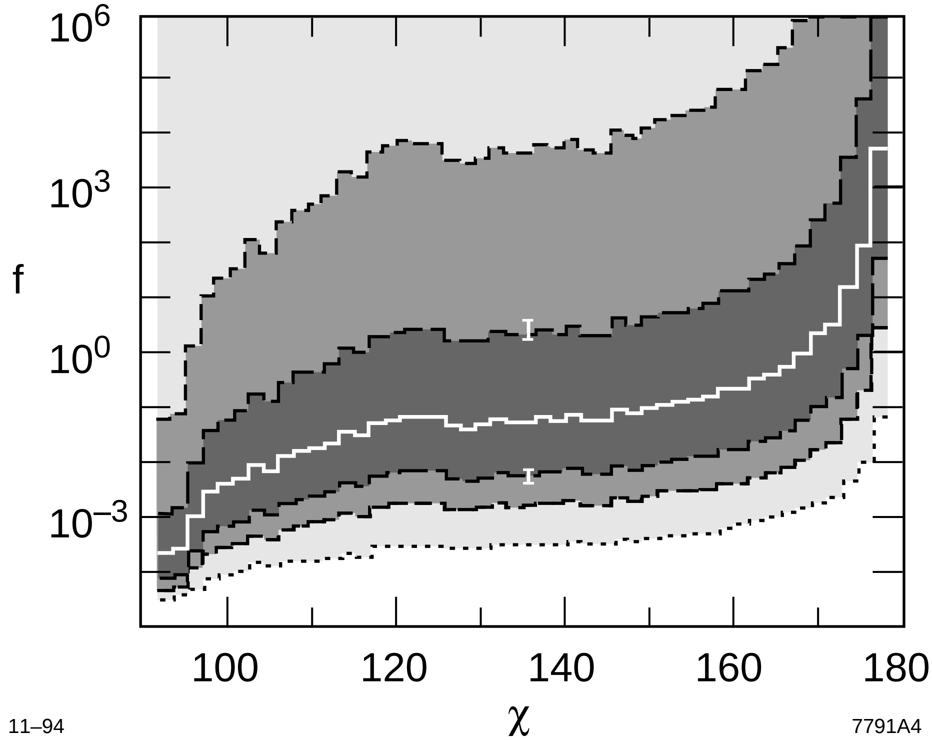

Fig. 4